Inorg. Chem. **2002**, *41*, 6597−6603

Synthesis, Structure, and Second-Order Nonlinear Optical Properties of Copper(II) and Palladium(II) Acentric Complexes with *N*-Salicylidene-*N′*-aroylhydrazine Tridentate Ligands

F. Cariati,[†] U. Caruso,[‡] R. Centore,*[,‡] W. Marcolli,[†,§] A. De Maria,[‡] B. Panunzi,[||] A. Roviello,*[,‡] and A. Tuzi[‡]

Dipartimento di Chimica, Università degli Studi di Napoli "Federico II", Via Cinthia, 80126 Napoli, Italy, Dipartimento di Chimica Inorganica, Metallorganica ed Analitica, Università degli Studi di Milano, Via Venezian 21, 20133 Milano, Italy, Consorzio Interuniversitario Nazionale per la Scienza e Tecnologia dei Materiali, Via B. Varchi 59, 50132 Firenze, Italy, and Dipartimento di Scienza degli Alimenti, Università degli Studi di Napoli "Federico II", Via Università 100, 80055 Napoli, Italy

Received February 14, 2002

Two new *N*-salicylidene-*N′*-aroylhydrazines ligands have been prepared: *N*-4-diethylaminosalicylidene-*N′*-4-nitrobenzoyl-hydrazine (L_1) and *N*-4-diethylaminosalicylidene-*N′*-4-(4-nitrophenylethylidene)-benzoyl-hydrazine (L_2). The ligands are properly functionalized with strong electron donor−acceptor groups and are of potential interest in second-order nonlinear optics (NLO). Dimeric copper(II) and palladium(II) complexes with L_1 and L_2 have been prepared, and, starting from these, mononuclear acentric adducts with pyridine as a further ligand have been prepared and characterized. The X-ray structures of three adducts are also reported. The NLO activity of the adducts has been determined by EFISH measurements giving $\mu\beta$ values up to 1500×10^{-48} esu for an incident wavelength of 1.907 μm.

Introduction

Metal coordination has been used in several ways to improve the behavior of all organic push−pull chromophores for applications in second-order nonlinear optics (NLO). The most common approach is the use of organometallic or metal coordinated fragments attached at the end of organic π conjugated systems: proper choice of the metal and its oxidation state and of the ligands allows the fragment to behave as an electron donor or acceptor group.[1] In some cases metals have been used as cations involved in ionic bonds with negatively charged conjugated π systems giving non-centrosymmetric crystals (phenate or carboxylate salts).[2−4] Another possibility is using metals as conjugation bridges along a push−pull organic system. In that case, the choice of metals that give planar coordination geometry may force a coplanar arrangement of the organic skeleton, so improving conjugation and, possibly, NLO properties.[5,6]

The step toward a NLO material is based on the inclusion of the NLO active molecules (chromophores) within a polymer matrix; this may be performed without covalent bonding (guest−host systems) or with. In the latter case NLO active fragments of the polymer chain are oriented under a strong electric field by heating the polymer above the glass transition temperature (poling) and the orientation is frozen by cooling the poled polymer below the glass transition.[7]

[†] Università degli Studi di Milano.
[‡] Dipartimento di Chimica, Università degli Studi di Napoli "Federico II".
[§] Consorzio Interuniversitario Nazionale per la Scienza e Tecnologia dei Materiali.
[||] Dipartimento di Scienza degli Alimenti, Università degli Studi di Napoli "Federico II".
* Authors for correspondence. E-mail: centore@chemistry.unina.it (R.C.); roviello@chemistry.unina.it (A.R.).

(1) Whittall, I. R.; McDonagh, A. M.; Humphrey, M. G.; Samoc, M. *Adv. Organomet. Chem.* **1998**, *42*, 291−361 and references therein.
(2) Minemoto, H.; Sonoda, N.; Miki, K. *Acta Crystallogr.* **1992**, C*48*, 737−738.
(3) Brahadeeswaran, S.; Venkataramanan, V.; Sherwood, J. N.; Bhat, H. L. *J. Mater. Chem.* **1998**, *8*, 613−618.
(4) Centore, R.; Tuzi, A. *Acta Crystallogr.* **2001**, C*57*, 698−701.
(5) Buey, J.; Coco, S.; Diez, L.; Espinet, P.; Martin-Alvarez, J. M.; Miguel, J. A.; Garcia-Granda, S.; Tesoro, A.; Ledoux, I.; Zyss, J. *Organometallics* **1998**, *17*, 1750−1755.
(6) Centore, R.; Panunzi, B.; Roviello, A.; Tuzi, A. *Acta Crystallogr.* **2002**, C*58*, m26−m28.
(7) Dalton, L.; Harper, A.; Ren, A.; Wang, F.; Todorova, G.; Chen, J.; Zhang, C.; Lee, M. *Ind. Eng. Chem. Res.* **1999**, *38*, 8−33.

10.1021/ic020127k CCC: $22.00
Published on Web 11/14/2002

Scheme 1

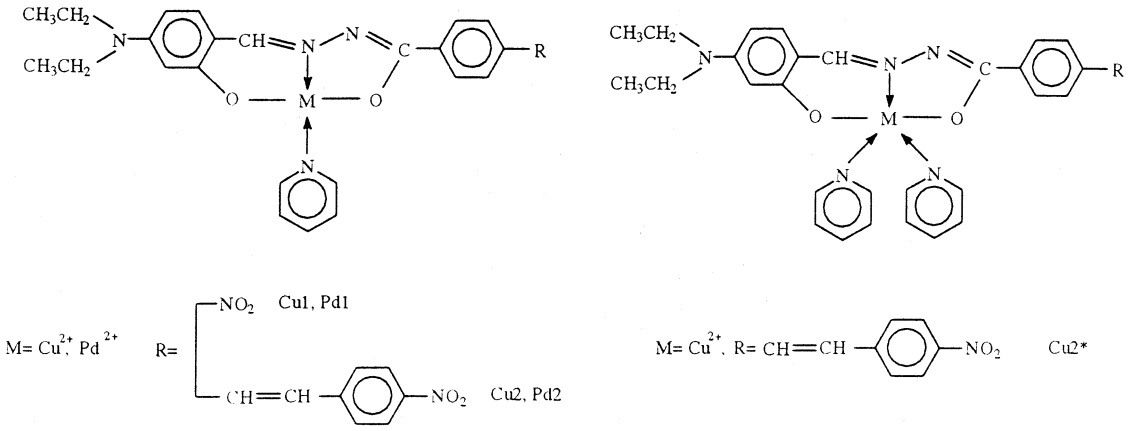

Scheme 2

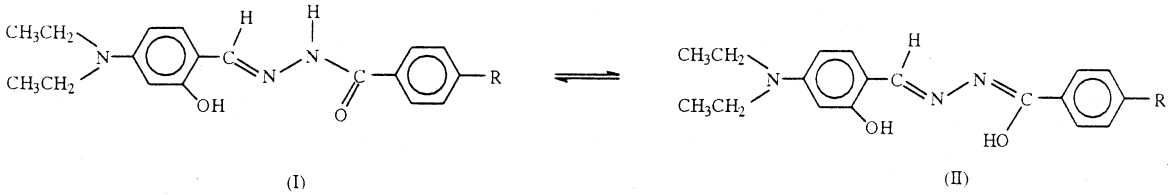

In the present paper we report the synthesis and characterization, including NLO measurements, of some [(*N*-salicylidene-N′-aroylhydrazine) *ONO* (pyridine)] Cu(II) and Pd(II) complexes of potential interest in second-order NLO, as depicted in Scheme 1.

N-Aroyl-*N*-salicylidene-hydrazine copper (II) complexes and their adducts with monodentate neutral Lewis bases have been studied up to now for biological and magnetic properties.[8−10]

In the present compounds the organic tridentate ligand has been properly functionalized with strong electron donor acceptor groups, this making them of potential interest in second-order NLO. Furthermore, these compounds have some peculiarities with respect to the above-described approaches for generating NLO active metal coordinated materials that are worth being briefly summarized.

First of all the ligand alone is not expected to show a high NLO activity because its electronic structure should be in the keto (amide) form (I, Scheme 2) with rather low conjugation from the dialkylamino donor to the nitro acceptor group. Upon coordination to the metal, the electronic structure of the ligand changes in the enolic form (II) with increase in the conjugation and, hence, in NLO activity.

Therefore, in this case, the primary role played by the metal is that of generating the actual push−pull chromophore. Furthermore, the use of square planar coordinating metals (Cu(II) or Pd(II)) should force the organic ligand in a planar conformation so as to maximize conjugation.

Second, the metal coordinated to the ligand is electrically neutral but coordinatively unsaturated. This means that further coordination with donor atoms is possible (N atom of the coordinated pyridine in the reported compounds); this feature, which is well-known in this class of complexes,[8] is particularly attractive in our case, since the donor atom might belong to a polymer matrix, this allowing automatically the covalent anchorage of the NLO active organometallic fragments to a preformed polymer chain. We have explored successfully this possibility using commercial poly(4-vinylpyridine).[11]

Experimental Section

Synthesis. Compounds Cu1, Cu2, Cu2*, Pd1, and Pd2 were synthesized according to the general procedure depicted in Scheme 3 starting with the synthesis of the organic ligands (L_1 and L_2), followed by the synthesis of the dinuclear complexes $(CuL_1)_2$, $(PdL_1)_2$, $(CuL_2)_2$, and $(PdL_2)_2$ and, from these, of the final compounds.

Synthesis of L_1. *N*-4-Diethylaminosalicylidene-*N*′-4-nitrobenzoyl-hydrazine. 4-Nitrobenzoyl hydrazide (9.06 g, 0.050 mol) and 9.26 g (0.050 mol) of 4-*N*,*N*-diethylamino-2-hydroxybenzaldehyde are dissolved in 70 mL of DMF. The solution is heated to boiling for 5 min and then is cooled to room temperature and poured into 400 mL of water containing crushed ice and 8 mL of concentrated sulfuric acid. The formed red solid is recovered by filtration, washed repeatedly with water, and recrystallized from DMF/water. Yield: 12.47 g (70%). Mp: 230 °C.

^{1}H NMR (DMSO-d_6) δ (ppm): 1.07 (m, 6H); 3.31 (m, 4H); 6.09 (s, 1H); 6.30 (d, 1H, J = 8.79 Hz); 7.20 (dd, 1H, J_1 = 8.79 Hz, J_2 = 3.42 Hz); 8.18 (m, 2H); 8.37 (m, 3H); 11.25 (s, 1H); 12.04 (s, 1H).

IR (KBr, cm^{-1}): 3366 (m), 3187 (w, N−H str), 2976 (m), 2934 (w), 1631 (vs, C═O str), 1594 (vs, N−H bend), 1519 (vs), 1360 (s), 1342 (s), 1245 (m), 1134 (m), 706 (m).

UV−vis λ_{max} (nm), ϵ_{max} (dm^3 mol^{-1} cm^{-1}): 358, 2.3 × 10^4.

(8) Kato, M.; Muto, Y. *Coord. Chem. Rev.* **1988**, *92*, 45.
(9) Warda, S. A.; Dahlke, P.; Wocadlo, S.; Massa, W.; Friebel, C. *Inorg. Chim. Acta* **1998**, *268*, 117−124.
(10) Iskander, M. F.; Khalil, T. E.; Werner, R.; Haase, W.; Svoboda, I.; Fuess, H. *Polyhedron* **2000**, *19*, 1181−1191.
(11) Caruso, U.; De Maria, A.; Panunzi, B.; Roviello, A. *J. Polym. Sci., Part A: Polym. Chem.* **2002**, *40*, 2987−2993.

Scheme 3

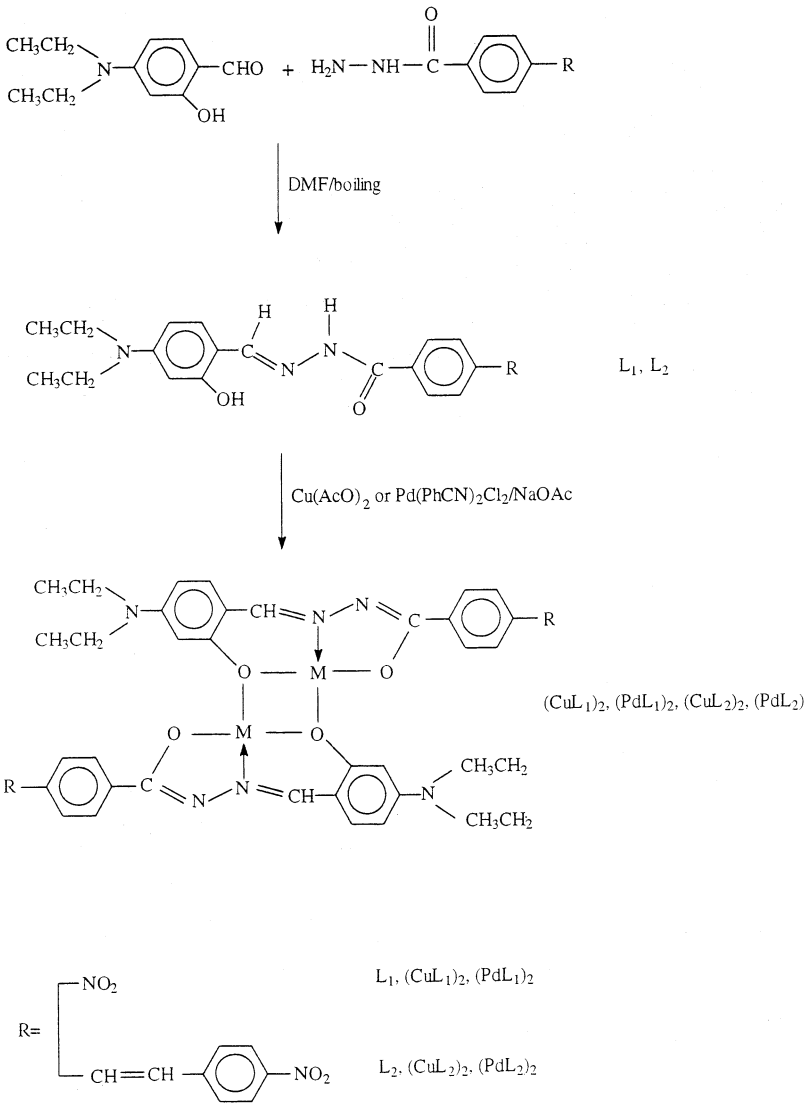

Synthesis of $(CuL_1)_2$. L_1 (0.40 g, 1.12 mmol), 0.22 g (1.12 mmol) of copper(II) acetate, and 0.50 g (6.10 mmol) of sodium acetate are suspended, under stirring, in hot absolute ethanol. After being stirred for 10 min, the formed dark red solid is recovered by filtration and recrystallized from DMF/water. Yield: 0.30 g (65%). Mp: 340 °C dec.

Anal. Calcd for $C_{36}H_{36}N_8O_8Cu_2$: C 51.74, H 4.55, N 13.41, Cu 15.21. Found: C 51.72, H 4.44, N 13.43, Cu 15.06.

UV−vis λ_{max} (nm), ϵ_{max} ($dm^3\ mol^{-1}\ cm^{-1}$): 460, 4.7×10^4.

Synthesis of $(PdL_1)_2$. L_1 (0.73 g, 2.05 mmol) is dissolved in 10 mL of THF at 50 °C. To this is added a solution obtained by dissolving 0.77 g (2.01 mmol) of bis(benzonitrile) Pd(II) dichloride in 15 mL of THF. A yellow suspension is formed to which sodium acetate (1.0 g dissolved in 20 mL of water) is added. A red solution is obtained, whose pH is raised to 9 by proper addition of KOH (pellets). After stirring for some minutes, 60 mL of water is added to the solution, affording the precipitation of a red-orange solid, which is filtered off, washed repeatedly with water, dried, and finally washed with boiling heptane. Yield: 0.63 g (67%). Mp: 280 °C dec.

Anal. Calcd for $C_{36}H_{36}N_8O_8Pd_2$: C 46.92, H 3.90, N 12.16, Pd 23.09. Found: C 46.73, H 4.12, N 12.19, Pd 23.65.

^{1}H NMR (DMSO-d_6) δ (ppm): 1.23 (m, 12H); 3.45 (m, 8H); 6.24 (s, 2H); 6.35 (d, 2H, $J = 8.79$ Hz); 7.43 (d, 2H, $J = 8.79$ Hz); 8.20 (m, 10H).

UV−vis λ_{max} (nm), ϵ_{max} ($dm^3\ mol^{-1}\ cm^{-1}$): 460, 3.6×10^4.

Synthesis of Cu1 and Pd1. In both cases 300 mg of the corresponding dinuclear precursor is dissolved in 5 mL of boiling pyridine. After 5 min the mononuclear complex is obtained by addition of water. The solid is recovered by filtration and recrystallized several times from pyridine/water. Final yields are about 75% in both cases.

Cu1. Anal. Calcd for $C_{23}H_{23}N_5O_4Cu$: C 55.58, H 4.66, N 14.09, Cu 12.79. Found: C 55.55, H 4.70, N 14.22, Cu 12.65.

UV−vis λ_{max} (nm), ϵ_{max} ($dm^3\ mol^{-1}\ cm^{-1}$): 460, 2.4×10^4.

Pd1. Anal. Calcd for $C_{23}H_{23}N_5O_4Pd$: C 51.17, H 4.29, N 12.97, Pd 19.71. Found: C 50.94, H 4.33, N 12.90, Pd 19.16.

^{1}H NMR ($CDCl_3$) δ (ppm): 1.19 (m, 6H), 3.37 (q, 4H, $J = 7.10$ Hz), 6.23 (d, 1H, $J = 8.79$ Hz), 6.39 (s, 1H), 7.25 (m, overlapped to solvent), 7.78 (m, 2H), 7.82 (s, 1H), 7.98 (t, 1H, $J = 7.33$ Hz), 8.21 (m, 4H), 9.30 (d, 2H, $J = 5.37$ Hz).

UV−vis λ_{max} (nm), ϵ_{max} ($dm^3\ mol^{-1}\ cm^{-1}$): 459, 2.5×10^4.

Synthesis of L_2. *N*-4-Diethylaminosalicylidene-*N′*-4-(4-nitrophenylethylidene)-benzoyl-hydrazine. 4-Nitrostilbene hydrazide

(6.86 g, 0.024 mol) and 4.80 g (0.025 mol) of 4-diethylamino-2-hydroxybenzaldehyde are dissolved in 50 mL of boiling DMF containing 0.5 mL of concentrated sulfuric acid. After 5 min of stirring, 5 mL of water is added. The orange solid formed is filtered, washed with water, and dried. Final recrystallization from DMF gives 8.25 g of the compound (75% yield). Mp: 286 °C.

^{1}H NMR (DMSO-d_6) δ (ppm): 1.07 (t, 6H, $J = 6.83$ Hz); 3.35 (m, 4H); 6.10 (s, 1H); 6.23 (d, 1H, $J = 8.79$ Hz); 7.16 (d, 1H, $J = 8.79$ Hz); 7.56 (s, 2H); 7.89 (m, 6H); 8.25 (d, 2H, $J = 8.79$ Hz); 8.41 (s, 1H); 11.45 (s, 1H); 11.80 (s, 1H).

IR (KBr, cm^{-1}): 3419 (m), 3225 (w, N−H str), 2975 (mw), 2931 (w), 1632 (vs, C═O str), 1591 (vs, N−H bend), 1519 (vs), 1341 (vs), 1248 (s), 1134 (s), 855 (m), 696 (m).

UV−vis λ_{max} (nm), ϵ_{max} (dm^3 mol^{-1} cm^{-1}): 380, 4.9×10^4.

Synthesis of $(CuL_2)_2$. L_2 (5.0 g, 0.011 mol), 2.2 g (0.011 mol) of copper(II) acetate, and 3.5 g (0.045 mol) of sodium acetate are dissolved in 120 mL of boiling DMF. After 10 min of stirring, the dark red solid formed is recovered by filtration and recrystallized from DMF/water. Yield: 3.43 g (60%). Mp: 335 °C dec.

UV−vis λ_{max} (nm), ϵ_{max} (dm^3 mol^{-1} cm^{-1}): 460, 7.8×10^4.

Anal. Calcd for $C_{52}H_{48}N_8O_8Cu_2$: C 60.06, H 4.61, N 10.78, Cu 12.22. Found: C 59.87, H 4.71, N 10.77, Cu 12.37.

Synthesis of $(PdL_2)_2$. L_2 (0.85 g, 1.86 mmol) is dissolved in 10 mL of THF at 50 °C. To this is added a solution obtained by dissolving 0.70 g (1.83 mmol) of bis(benzonitrile) Pd(II) dichloride in 15 mL of THF. A yellow suspension is formed to which sodium acetate (1.0 g dissolved in 20 mL of water) is added. A red solution is obtained, whose pH is raised to 9 by proper addition of KOH (pellets). After stirring for some minutes, 60 mL of water is added to the solution, affording the precipitation of a red-orange solid, which is filtered, washed repeatedly with water, dried, and finally washed with boiling heptane. Yield: 0.72 g (70%). Mp: 320 °C dec.

Anal. Calcd for $C_{52}H_{48}N_8O_8Pd_2$: C 55.47, H 4.30, N 10.00, Pd 18.90. Found: C 54.66, H 4.67, N 10.80, Pd 18.97.

^{1}H NMR (DMSO-d_6) δ (ppm): 1.07 (m, 12H); 3.29 (m, 8H); 6.14 (s, 2H); 6.22 (d, 2H, $J = 8.79$ Hz); 7.30 (d, 2H, $J = 8.79$ Hz); 7.55 (m, 8H); 7.87 (m, 10H); 8.19 (d, 4H, $J = 7.82$ Hz).

UV−vis λ_{max} (nm), ϵ_{max} (dm^3 mol^{-1} cm^{-1}): 450, 7.5×10^4.

Synthesis of Cu2* and Pd2. In both cases 300 mg of the corresponding dinuclear precursor are dissolved in 5 mL of boiling pyridine and stirred for 5 min. By cooling at room temperature crystals of complexes are formed and recovered by filtration. Yields are 77% in both cases.

Cu2*. Anal. Calcd for $C_{36}H_{34}N_6O_4Cu$: Cu 9.37. Found: 9.43.

Pd2. Anal. Calcd for $C_{31}H_{29}N_5O_4Pd$: C 58.00, H 4.55, N 10.91, Pd 16.58. Found: C 57.84, H 4.53, N 10.99, Pd 17.03.

^{1}H NMR (CD_2Cl_2) δ (ppm): 1.23 (m, 6H); 3.40 (q, 4H, $J = 7.10$ Hz); 6.25 (d, 1H, $J = 8.79$ Hz); 6.39 (s, 1H); 7.25 (d, 1H, $J = 8.79$ Hz); 7.31 (d, 2H, $J = 6.81$ Hz), 7.65 (m, 7H); 8.14 (t, 1H, $J = 7.33$ Hz); 8.18 (m, 4H), 9.03 (d, 2H, $J = 5.37$ Hz).

UV−vis λ_{max} (nm), ϵ_{max} (dm^3 mol^{-1} cm^{-1}): 450, 4.1×10^4.

Synthesis of Cu2. Cu2 was obtained by thermal treatment of Cu2* in an oven at 120 °C for 2 h.

Cu2. Anal. Calcd for $C_{31}H_{29}N_5O_4Cu$: C 62.15, H 4.88, N 11.69, Cu 10.61. Found: C 61.88, H 4.86, N 11.74, Cu 10.67.

UV−vis λ_{max} (nm), ϵ_{max} (dm^3 mol^{-1} cm^{-1}): 455, 4.0×10^4.

Physical Measurements. The thermal behavior of compounds was examined by differential scanning calorimetry (Perkin-Elmer DSC-7, nitrogen atmosphere, scanning rate 10 K/min), temperature controlled polarizing microscopy (Zeiss microscope combined with a Mettler FP5 microfurnace, scanning rate 10 K/min, glass slides), and combined TGA-DTA analysis (TA Instruments SDT 2960, air atmosphere, scanning rate 10 K/min). Proton NMR spectra were recorded on a Varian XL 200 and Bruker MW 400 spectrometers. UV−vis spectra were recorded with a Perkin-Elmer Lambda 7 UV−vis spectrophotometer. IR spectra were recorded from KBr pellets on a FT-IR JASCO spectrometer.

X-ray Analysis. Single crystals suitable for X-ray analysis were obtained by slow evaporation, at ambient temperature, of a pyridine solution for Cu1; for Pd1 they were grown from a hot pyridine/ethanol/water solution (70/30/10 vv) by slow cooling at 4 °C; for Cu2*, single crystals were obtained from a saturated pyridine solution at 100 °C by slow cooling.

Accurate cell parameters were obtained through a least-squares fit to the setting angles of 25 accurately centered strong reflections in the ranges $12.10° \le \theta \le 13.42°$ for Cu1, $12.19° \le \theta \le 13.96°$ for Pd1, and $11.92° \le \theta \le 15.72°$ for Cu2* on an Enraf-Nonius MACH 3 automated single-crystal diffractometer, using graphite-monochromated Mo Kα radiation ($\lambda = 0.71069$ Å). Data collection was performed on the same apparatus in the ω/θ scan mode. In all cases crystal specimens remained stable during data collection as confirmed by the intensity of control reflections periodically measured, which showed only random fluctuations. Semiempirical absorption correction (ψ scans) was applied in all cases. The structures were solved by direct methods (SHELXS program of SHELX 97 package[12]), completed by difference Fourier methods and refined by the full matrix least-squares method (SHELXL program of the same package). Refinement was on F^2 against all independent measured reflections; σ weights were introduced in the last refinement cycles. The largest peaks and holes in the last Fourier difference were (e Å^{-3}) 0.426 and −0.454 for Cu1, 0.673 and −0.690 for Pd1, and 0.858 and −0.766 for Cu2*. In all structures C, O, N, and metal atoms were given anisotropic displacement parameters. H atoms were placed in calculated positions and refined by the riding model with U_{iso} equal to U_{eq} of the carrier atoms. In the case of Cu1 one of the ethyl groups is disordered on two sites corresponding to the two common geometries found for the diethylamino group, i.e., binary symmetry around the N to phenyl bond and mirror symmetry through the plane perpendicular to the phenyl and containing the N to phenyl bond. The two sites were handled with 0.5 occupation factor without introducing constraints. A search in the April 2001 release of the CSD file[13] has given three cases of identical disorder.[14−16] H atoms of the water molecule in Pd1 have not been considered. Some crystal, collection, and refinement data are reported in Table 1.

NLO Measurements. Measurements of second-order nonlinear optical properties were performed by the EFISH (electric field induced second harmonic generation) technique.[17]

Measurements were carried out in DMSO or in chloroform solutions at a fundamental wavelength of 1.907 μm, using a Q-switched, mode locked Nd^{3+}:YAG laser with pulse durations of 15 ns at a 10 Hz repetition rate, whose 1.064 μm initial wavelength was shifted by stimulated Raman scattering in a high-pressure hydrogen cell.

(12) Sheldrick, G. M. *SHELX-97*; University of Göttingen: Göttingen, Germany, 1997.
(13) *CSD April 2001 release*; Cambridge Crystallographic Data Centre: Cambridge, England, 2001.
(14) Maurin, J. K. *Pol. J. Chem.* **1988**, *62*, 857. CSD refcode FUGTIK01.
(15) Suchod, B.; Baldeck, P. *Acta Crystallogr.* **1995**, *C51*, 432−434. CSD refcode WINLUA.
(16) Kliegel, W.; Metge, J.; Rettig, S. J.; Trotter, J. *Can. J. Chem.* **1998**, *76*, 1082−1092. CSD refcode BIBQEI.
(17) Ledoux, I.; Zyss, J., *J. Chem. Phys.* **1982**, *73*, 203.

Table 1. Crystal, Collection and Refinement Data for Cu1, Pd1, and Cu2*

	Cu1	Pd1	Cu2*
chem formula	$C_{23}H_{23}N_5O_4Cu$	$C_{23}H_{23}N_5O_4Pd\cdot0.25H_2O$	$C_{36}H_{34}N_6O_4Cu$
fw	497.01	544.39	678.23
T (K)	293	293	293
cryst syst	triclinic	orthorhombic	triclinic
space group	$P\bar{1}$	*Pbcn*	$P\bar{1}$
a (Å)	8.576(4)	24.507(3)	12.219(2)
b (Å)	11.143(6)	10.092(5)	13.831(1)
c (Å)	12.990(5)	37.047(9)	20.948(6)
α (deg)	104.44(4)	90	83.77(2)
β (deg)	104.94(5)	90	77.98(2)
γ (deg)	103.58(4)	90	70.66(1)
V (Å^3)	1100.6(9)	9163(5)	3264(1)
Z, D_x (g/cm^3)	2, 1.500	16, 1.577	4, 1.380
μ (mm^{-1})	1.033	0.851	0.718
θ range (deg)	1.72−29.96	1.10−27.98	1.56−27.98
data/params	6392/316	11040/600	15702/847
R1, wR2 on F ($I > 2\sigma(I)$)[a]	0.0513, 0.1389	0.0681, 0.1224	0.0682, 0.1406
R1, wR2 (all data) on F^2	0.1354, 0.1649	0.2960, 0.197	0.2394, 0.1879

[a] $R1 = [\sum||F_o| - |F_c||]/\sum|F_o|$; $wR2 = \{[\sum[w(F_o^2 - F_c^2)^2]]/\sum[w(F_o^2)^2]\}^{1/2}$.

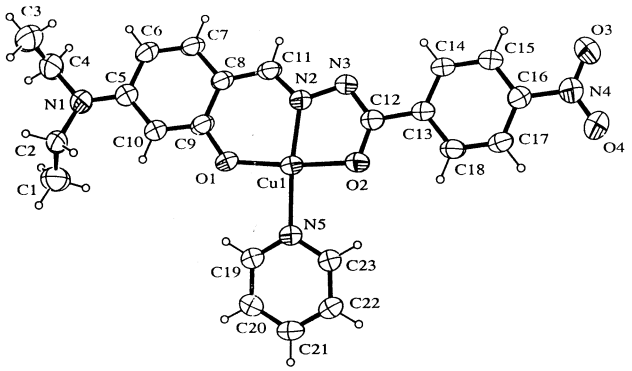

Figure 1. Cu1. Crystallographically independent molecule.

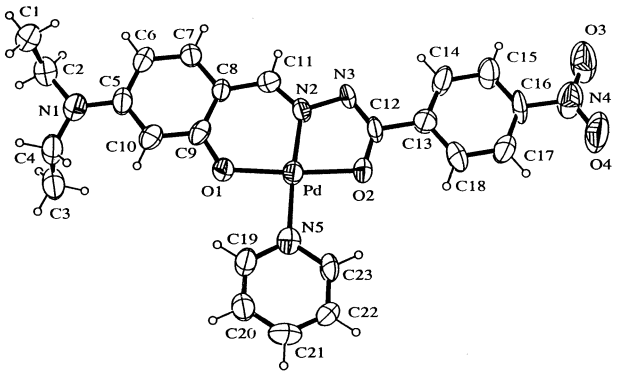

Figure 2. Pd1. Crystallographically independent molecule A.

Results and Discussion

Drawings of the crystallographically independent units of Cu1, Pd1, and Cu2* are reported in Figures 1−5. Selected bond lengths, bond angles, and torsion angles are reported in Table 2. A fair agreement among corresponding structural data of the five molecular structures within the three crystal structures is observed. In particular, in Pd1 the two crystallographically independent molecules almost only differ because molecule B is involved in hydrogen bonding with the water molecule (N3···OW = 2.89(1) Å).

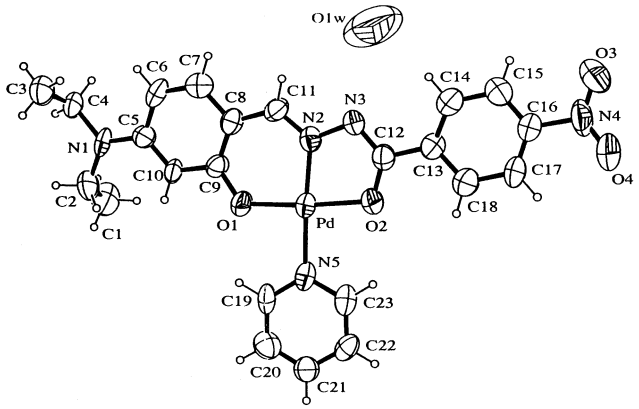

Figure 3. Pd1. Crystallographically independent molecule B.

A common feature is given by the structure of the tridentate ligand which is in the enolic form. This is clearly shown by the increase in the length of C12−O2 bond which ranges between 1.286(5) and 1.31(1) Å as compared to the value expected for an amide carbonyl group (1.23 Å[18]) and shortening of C12−N3 which ranges between 1.29(1) and 1.320(6) Å. The structure of free ligands L_1 and L_2, on the other hand, is in the keto form as clearly evidenced by the IR data showing, among other indicative bands, the C═O stretching and N−H bending bands (amide I and amide II bands). The change in the electronic structure of ligands is also consistent with the UV−vis data showing a significant red shift of the λ_{max} upon coordination. Furthermore, among dimeric complexes and monoadducts λ_{max} is substantially unchanged while the molar extinction coefficient is almost doubled, as expected.

To our knowledge organic ligands L_1 and L_2 are the first reported examples of hydrazine-based, donor−acceptor derivatives.

The geometry around the N1 amino atom is planar in all the compounds. Shortening of the N to phenyl distance, which ranges between 1.361(6) and 1.38(1) Å in the five molecular structures, as compared to the value of 1.43 Å reported for pyramidal N,[18] is indicative of π conjugation from the lone pair of N1 to the adjacent phenyl ring.

The conformation of the organic fragment is substantially planar. For the tridentate part of the ligand, planarity is imposed by the coordination geometry. However, in the two independent molecules of Cu2* a substantially planar arrangement is observed also for the stilbene moiety which is not involved in coordination.

The coordination geometry is substantially square planar, as expected, in Cu1 and Pd1 with trans arrangement of N and O atoms around the metal and the plane of the pyridine molecule being substantially coplanar with the metal coordination plane. In Cu2* a different geometry is observed, as metal atoms are bonded to five coordinating atoms and, in particular, two pyridine molecules are coordinated to the metal. Although evidence of the possibility of further coordination of a nitrogen ligand to Cu (II) monoadducts

(18) Allen, F. H.; Kennard, O.; Watson, D. G.; Brammer, L.; Guy Orpen, A.; Taylor, R. *J. Chem. Soc., Perkin Trans. 2* **1987** S1−S19.

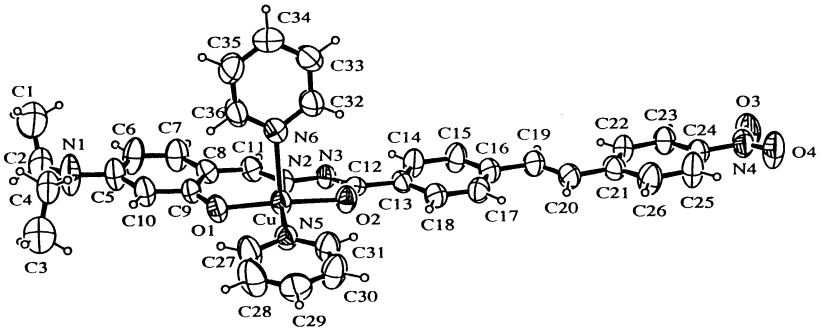

Figure 4. Cu2*. Crystallographically independent molecule A.

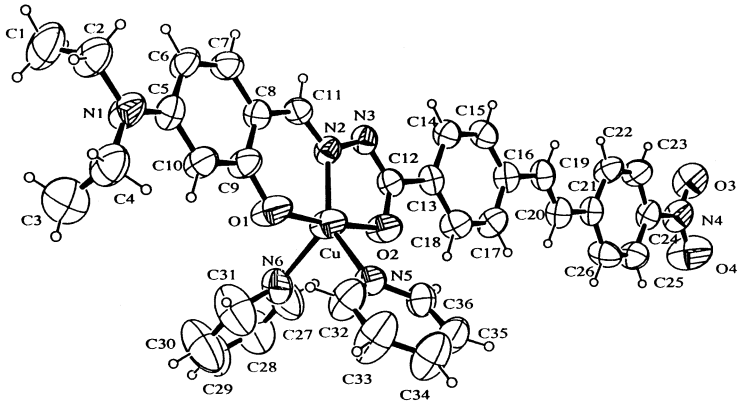

Figure 5. Cu2*. Crystallographically independent molecule B.

Table 2. Selected Bond Lengths (Å), Bond Angles (deg), and Torsion Angles (deg)

		Pd1		Cu2*	
	Cu1	A	B	A	B
M−O1	1.881(3)	1.969(6)	1.977(6)	1.920(3)	1.907(3)
M−O2	1.926(3)	1.990(6)	2.009(6)	1.962(3)	1.948(3)
M−N2	1.914(3)	1.927(7)	1.931(7)	1.921(4)	1.918(4)
M−N5	2.006(3)	2.037(7)	2.063(8)	2.005(4)	2.088(4)
M−N6				2.354(4)	2.243(5)
O2−C12	1.293(4)	1.30(1)	1.31(1)	1.286(5)	1.294(5)
N1−C5	1.362(5)	1.38(1)	1.37(1)	1.361(6)	1.372(6)
N2−C11	1.294(4)	1.30(1)	1.32(1)	1.287(5)	1.283(5)
N2−N3	1.395(4)	1.406(9)	1.39(1)	1.393(5)	1.403(5)
N3−C12	1.317(4)	1.29(1)	1.31(1)	1.320(6)	1.301(6)
C8−C11	1.418(5)	1.40(1)	1.43(1)	1.420(6)	1.427(6)
C12−C13	1.481(5)	1.47(1)	1.46(1)	1.479(6)	1.481(6)
O1−M−N2	93.8(1)	94.2(3)	95.1(3)	93.3(2)	93.4(2)
N2−M−O2	81.4(1)	80.8(3)	80.2(3)	80.0(1)	80.7(2)
O1−M−N5	92.3(1)	90.4(3)	88.7(3)	92.9(2)	91.4(2)
O2−M−N5	93.6(1)	94.7(3)	96.0(3)	92.6(1)	92.3(2)
N2−M−N5				166.0(2)	119.6(2)
N2−M−N6				97.0(2)	144.3(2)
N5−M−N6				95.4(2)	95.6(2)
C2−N1−C4	115.4(5)−112.4(5)	115.6(9)	115.8(8)	116.3(5)	116.9(4)
C2−N1−C5	118.2(5)−121.9(5)	121.9(9)	121.4(9)	121.2(5)	121.5(5)
C4−N1−C5	123.1(3)	122.4(9)	122.7(9)	122.4(5)	121.5(4)
C11−N2−N3−C12	178.0(3)	179.2(9)	177.0(9)	172.1(4)	177.4(4)
C7−C8−C11−N2	−179.8(3)	178.4(9)	−179(1)	178.1(5)	178.5(4)
N3−C12−C13−C18	−178.8(3)	−176(1)	178(1)	−173.3(4)	−174.9(4)
C15−C16−C19−C20				−176.3(6)	−166.1(5)
C16−C19−C20−C21				−177.4(5)	177.4(5)
C19−C20−C21−C26				171.7(6)	176.4(5)

has already been given in the literature,[19,20] to our knowledge this is the first direct crystallographic evidence of that behavior. Furthermore, different coordination geometries are observed in the two crystallographically independent molecules of Cu2*.

In molecule A a square pyramidal geometry is observed, with the metal atom almost lying in the basal plane. Bond distances between the metal and two coordinated pyridine molecules are significantly different. The bond length with basal pyridine is clearly shorter than the length with that out of the basal plane, this meaning that the second pyridine is more weakly bonded and may become lost easily.

In molecule B the geometry is substantially trigonal bipyramidal, with the three coordinated N atoms belonging to the equatorial plane, the two O atoms being apical, and the planes of the two pyridine molecules being almost parallel to the O1−O2 direction (axis of the bipyramid). Also in this case bond lengths between Cu and N atoms of the two coordinated pyridine molecules are significantly different.

The results of combined TGA−DTA analysis are consistent with the crystal structure analysis. As an example, in Figure 6, which reports TGA−DTA curves for Cu2*, it is clearly shown that the first pyridine molecule is lost near 100 °C while the second is lost near 180 °C. In the case of Cu1 loss of the only pyridine molecule occurs near 170 °C, giving a product whose TGA−DTA curves are identical to those of the corresponding dinuclear complex, $(CuL_1)_2$. This behavior is consistent with literature data suggesting that thermal loss of the pyridine should correspond to restoring of dinuclear complexes.[19] For Pd complexes, on the other hand, the temperature ranges for loss of pyridine are broader, not so well defined, and in some cases partially superimposed with thermal degradation of the compound.

(19) Iskander, M. F.; El-Aggan, A. M.; Refaat, L. S.; El Sayed, L. *Inorg. Chim. Acta* **1975**, *14*, 167−172.
(20) Jezierska, J.; Jezierski, A.; Jezowska-Trzebiatowska, B.; Ozarowsky, A. *Inorg. Chim. Acta* **1983**, *68*, 7−13.

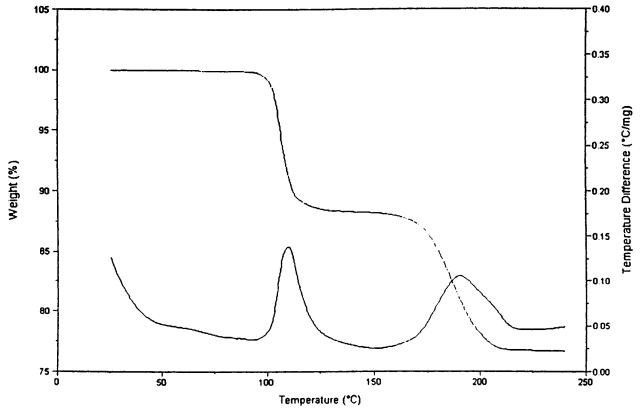

Figure 6. TGA−DTA curves for Cu2*.

Table 3. EFISH Results for the Studied Complexes

compd	$\mu\beta_{vec}$ (10^{-48} esu)	solvent
Cu1	+460	DMSO
Pd1	+380	chloroform
Cu2[a]	+650	DMSO
Cu2*	+1390	chloroform
Pd2	+1500	DMSO

[a] In this case the measurement was performed on a sample of Cu2* crystals after loss of the more weakly bounded pyridine molecule (treatment in oven at 120 °C).

The results of EFISH measurements are shown in Table 3. We note that the measured values are consistent with the expected increase of the NLO activity in going from L_1 to L_2 ligand, on account of the increase of the conjugation length. In fact, it is known that pseudolinear π-delocalized organic systems substituted by donor and acceptor groups at the two ends show significant second-order NLO responses due to a reduced energy gap between ground and intramolecular charge-transfer excited states, together with large oscillator strengths and a significant difference between ground and excited-state dipole moments.[21] Furthermore the values are comparable to or even higher than those reported, under similar experimental conditions, for DR (Disperse Red) chromophore,[7] which is the up to date reference for possible NLO applications of organic polymers.[22]

Actually the reported values should be considered as lower limits because a partial restoring of dinuclear complexes through solution equilibria, which are dependent on the nature of the metal but also of the ligand and the solvent, would give a reduced contribution to $\mu\beta_{vec}$ as they are centrosymmetric and, hence, not NLO active; furthermore evidence of the possibility of centrosymmetric coupling also of monoadducts has been reported.[9,10] The strongly reduced $\mu\beta_{vec}$ value measured for a sample of Cu2* after loss of the more weakly bounded pyridine molecule (i.e., for a sample of Cu2) could point to this possibility.

Some of the features discussed above are of potential interest within the approach depicted in the Introduction for obtaining NLO active polymer materials based on these complexes. In particular the possibility of coordination of a second pyridine molecule to metal atoms is noteworthy as it could act as a partial networking of the polymer structure with further constraint of the NLO active fragments. In conclusion, the system should couple, at least partially, the advantages of guest−host systems (higher mobility of NLO active fragments and, hence, higher degree of orientation during the poling) with those of truly covalent systems (better time stability of the polar orientation).

Acknowledgment. Financial support of PRIN 2000 (Italy) is gratefully acknowledged. Thanks are due to the Centro Interdipartimentale di Metodologie Chimico-Fisiche of the Università di Napoli "Federico II" for NMR, X-ray (MACH3 Nonius diffractometer) and CSD facilities. Thanks are also due to CIRA (Centro Italiano di Ricerche Aerospaziali) for TGA−DTA measurements.

Supporting Information Available: Crystallographic data in CIF format. This material is available free of charge via the Internet at http://pubs.acs.org.

IC020127K

(21) Ledoux, I.; Zyss, J. Molecular Nonlinear Optics: Fundamentals and Applications. In *Novel Optical Materials and Applications*; Khoo, I. C., Simoni, F., Umeton, C., Eds.; John Wiley & Sons: New York, 1977.

(22) Pliška, T.; Cho, W.-R.; Meier, J.; Le Duff, A.-C.; Ricci, V.; Otomo, A.; Canva, M.; Stegeman, G. I.; Raimond, P.; Kajzar, F. *J. Opt. Soc. Am. B* **2000**, *17* (9), 1554−1564.